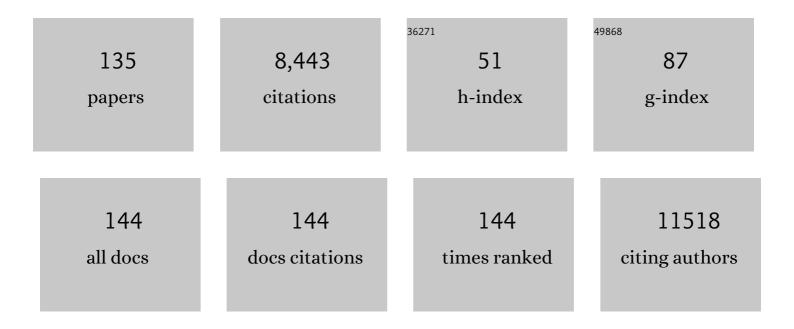
List of Publications by Year in descending order

Source: https://exaly.com/author-pdf/7340415/publications.pdf Version: 2024-02-01



ZUENLI

#	Article	IF	CITATIONS
1	One-pot solventless preparation of PEGylated black phosphorus nanoparticles for photoacoustic imaging and photothermal therapy ofÂcancer. Biomaterials, 2016, 91, 81-89.	5.7	403
2	Charge-Controlled Switchable CO ₂ Capture on Boron Nitride Nanomaterials. Journal of the American Chemical Society, 2013, 135, 8246-8253.	6.6	293
3	Ambient Aqueous Synthesis of Ultrasmall PEGylated Cu _{2â^'} <i>_x</i> Se Nanoparticles as a Multifunctional Theranostic Agent for Multimodal Imaging Guided Photothermal Therapy of Cancer. Advanced Materials, 2016, 28, 8927-8936.	11.1	282
4	BSAâ€Mediated Synthesis of Bismuth Sulfide Nanotheranostic Agents for Tumor Multimodal Imaging and Thermoradiotherapy. Advanced Functional Materials, 2016, 26, 5335-5344.	7.8	255
5	Ultrasmall Biocompatible WO _{3â^'} <i>_x</i> Nanodots for Multiâ€Modality Imaging and Combined Therapy of Cancers. Advanced Materials, 2016, 28, 5072-5079.	11.1	227
6	In Situ Growth of a ZnO Nanowire Network within a TiO ₂ Nanoparticle Film for Enhanced Dye‣ensitized Solar Cell Performance. Advanced Materials, 2012, 24, 5850-5856.	11.1	218
7	A facile vesicle template route to multi-shelled mesoporous silica hollow nanospheres. Journal of Materials Chemistry, 2010, 20, 4595.	6.7	208
8	Unidirectional suppression of hydrogen oxidation on oxidized platinum clusters. Nature Communications, 2013, 4, 2500.	5.8	197
9	Ultrasmall Biocompatible Bi ₂ Se ₃ Nanodots for Multimodal Imaging-Guided Synergistic Radiophotothermal Therapy against Cancer. ACS Nano, 2016, 10, 11145-11155.	7.3	196
10	Ultra-thin anatase TiO ₂ nanosheets dominated with {001} facets: thickness-controlled synthesis, growth mechanism and water-splitting properties. CrystEngComm, 2011, 13, 1378-1383.	1.3	189
11	Ultrasmall Waterâ€Soluble and Biocompatible Magnetic Iron Oxide Nanoparticles as Positive and Negative Dual Contrast Agents. Advanced Functional Materials, 2012, 22, 2387-2393.	7.8	181
12	Ultrasmall Magnetic CuFeSe ₂ Ternary Nanocrystals for Multimodal Imaging Guided Photothermal Therapy of Cancer. ACS Nano, 2017, 11, 5633-5645.	7.3	181
13	Boosting H ₂ O ₂ â€Guided Chemodynamic Therapy of Cancer by Enhancing Reaction Kinetics through Versatile Biomimetic Fenton Nanocatalysts and the Second Nearâ€Infrared Light Irradiation. Advanced Functional Materials, 2020, 30, 1906128.	7.8	177
14	Thermoelectric Enhancement of Different Kinds of Metal Chalcogenides. Advanced Energy Materials, 2016, 6, 1600498.	10.2	145
15	Direct Coprecipitation Route to Monodisperse Dualâ€Functionalized Magnetic Iron Oxide Nanocrystals Without Size Selection. Small, 2008, 4, 231-239.	5.2	137
16	Photoreductive synthesis of water-soluble fluorescent metal nanoclusters. Chemical Communications, 2012, 48, 567-569.	2.2	133
17	Facile Synthesis of Highly Efficient One-Dimensional Plasmonic Photocatalysts through Ag@Cu ₂ O Core–Shell Heteronanowires. ACS Applied Materials & Interfaces, 2014, 6, 15716-15725.	4.0	127
18	Recent progress in thermoelectric materials. Science Bulletin, 2014, 59, 2073-2091.	1.7	113

#	Article	IF	CITATIONS
19	Monitoring the Opening and Recovery of the Blood–Brain Barrier with Noninvasive Molecular Imaging by Biodegradable Ultrasmall Cu _{2–<i>x</i>} Se Nanoparticles. Nano Letters, 2018, 18, 4985-4992.	4.5	105
20	Ultra-small fluorescent inorganic nanoparticles for bioimaging. Journal of Materials Chemistry B, 2014, 2, 2793-2818.	2.9	104
21	Second near-infrared photodynamic therapy and chemotherapy of orthotopic malignant glioblastoma with ultra-small Cu _{2â^x} Se nanoparticles. Nanoscale, 2019, 11, 7600-7608.	2.8	100
22	Engineering NIR-IIb fluorescence of Er-based lanthanide nanoparticles for through-skull targeted imaging and imaging-guided surgery of orthotopic glioma. Nano Today, 2020, 34, 100905.	6.2	100
23	Targeting Microglia for Therapy of Parkinson's Disease by Using Biomimetic Ultrasmall Nanoparticles. Journal of the American Chemical Society, 2020, 142, 21730-21742.	6.6	97
24	Yolk@shell anatase TiO2 hierarchical microspheres with exposed {001} facets for high-performance dye sensitized solar cells. Journal of Materials Chemistry, 2012, 22, 22082.	6.7	96
25	Controlled synthesis of copper telluride nanostructures for long-cycling anodes in lithium ion batteries. Journal of Materials Chemistry A, 2014, 2, 11683.	5.2	94
26	pHâ€Responsive Fe(III)–Gallic Acid Nanoparticles for In Vivo Photoacousticâ€Imagingâ€Guided Photothermal Therapy. Advanced Healthcare Materials, 2016, 5, 772-780.	3.9	94
27	Boosting the Radiosensitizing and Photothermal Performance of Cu2–xSe Nanocrystals for Synergetic Radiophotothermal Therapy of Orthotopic Breast Cancer. ACS Nano, 2019, 13, 1342-1353.	7.3	91
28	Light-Enhanced O ₂ -Evolving Nanoparticles Boost Photodynamic Therapy To Elicit Antitumor Immunity. ACS Applied Materials & Interfaces, 2019, 11, 16367-16379.	4.0	90
29	A novel photoacoustic nanoprobe of ICG@PEG-Ag ₂ S for atherosclerosis targeting and imaging in vivo. Nanoscale, 2016, 8, 12531-12539.	2.8	84
30	Boosting often overlooked long wavelength emissions of rare-earth nanoparticles for NIR-II fluorescence imaging of orthotopic glioblastoma. Biomaterials, 2019, 219, 119364.	5.7	83
31	Ultra-small nanocluster mediated synthesis of Nd 3+ -doped core-shell nanocrystals with emission in the second near-infrared window for multimodal imaging of tumor vasculature. Biomaterials, 2018, 175, 30-43.	5.7	81
32	Ultrasmall Manganese Ferrite Nanoparticles as Positive Contrast Agent for Magnetic Resonance Imaging. Advanced Healthcare Materials, 2013, 2, 958-964.	3.9	80
33	Molecular imaging of activated platelets via antibody-targeted ultra-small iron oxide nanoparticles displaying unique dual MRI contrast. Biomaterials, 2017, 134, 31-42.	5.7	78
34	Electric field controlled CO ₂ capture and CO ₂ /N ₂ separation on MoS ₂ monolayers. Nanoscale, 2017, 9, 19-24.	2.8	78
35	Carbon Dioxide Capture and Gas Separation on B ₈₀ Fullerene. Journal of Physical Chemistry C, 2014, 118, 2170-2177.	1.5	77
36	Lead-free SnTe-based thermoelectrics: enhancement of thermoelectric performance by doping with Gd/Ag. Journal of Materials Chemistry A, 2016, 4, 7936-7942.	5.2	77

#	Article	IF	CITATIONS
37	Ambient Scalable Synthesis of Surfactant-Free Thermoelectric CuAgSe Nanoparticles with Reversible Metallic- <i>n-p</i> Conductivity Transition. Journal of the American Chemical Society, 2014, 136, 17626-17633.	6.6	76
38	Roomâ€Temperature Synthesis of Cu _{2â^'<i>x</i>} E (E=S, Se) Nanotubes with Hierarchical Architecture as Highâ€Performance Counter Electrodes of Quantumâ€Dotâ€Sensitized Solar Cells. Chemistry - A European Journal, 2015, 21, 1055-1063.	1.7	74
39	Robust Antibacterial Activity of Tungsten Oxide (WO _{3-x}) Nanodots. Chemical Research in Toxicology, 2019, 32, 1357-1366.	1.7	73
40	Boosting the efficiency of quantum dot sensitized solar cells up to 7.11% through simultaneous engineering of photocathode and photoanode. Nano Energy, 2015, 13, 609-619.	8.2	72
41	Glycocalyx-Mimicking Nanoparticles Improve Anti-PD-L1 Cancer Immunotherapy through Reversion of Tumor-Associated Macrophages. Biomacromolecules, 2018, 19, 2098-2108.	2.6	69
42	Aqueous synthesis of PEGylated copper sulfide nanoparticles for photoacoustic imaging of tumors. Nanoscale, 2015, 7, 11075-11081.	2.8	68
43	Biolabeling Hematopoietic System Cells Using Near-Infrared Fluorescent Gold Nanoclusters. Journal of Physical Chemistry C, 2011, 115, 16753-16763.	1.5	67
44	Functionalization of small black phosphorus nanoparticles for targeted imaging and photothermal therapy of cancer. Science Bulletin, 2018, 63, 917-924.	4.3	67
45	Ambient Facile Synthesis of Gram-Scale Copper Selenide Nanostructures from Commercial Copper and Selenium Powder. ACS Applied Materials & Interfaces, 2015, 7, 13295-13302.	4.0	65
46	Vacancy engineering of Cu _{2â^'x} Se nanoparticles with tunable LSPR and magnetism for dual-modal imaging guided photothermal therapy of cancer. Nanoscale, 2018, 10, 3130-3143.	2.8	64
47	Harnessing antiâ€ŧumor and tumorâ€ŧropism functions of macrophages via nanotechnology for tumor immunotherapy. Exploration, 2022, 2, .	5.4	64
48	One-pot synthesis of ultra-small magnetite nanoparticles on the surface of reduced graphene oxide nanosheets as anodes for sodium-ion batteries. Journal of Materials Chemistry A, 2015, 3, 4793-4798.	5.2	59
49	Aqueous preparation of surfactant-free copper selenide nanowires. Journal of Colloid and Interface Science, 2015, 442, 140-146.	5.0	58
50	Synthesis of Robust Sandwich-Like SiO ₂ @CdTe@SiO ₂ Fluorescent Nanoparticles for Cellular Imaging. Chemistry of Materials, 2012, 24, 421-423.	3.2	57
51	One-pot preparation of highly fluorescent cadmium telluride/cadmium sulfide quantum dots under neutral-pH condition for biological applications. Journal of Colloid and Interface Science, 2013, 390, 3-10.	5.0	53
52	Robust scalable synthesis of surfactant-free thermoelectric metal chalcogenide nanostructures. Nano Energy, 2015, 15, 193-204.	8.2	53
53	Manipulating solar absorption and electron transport properties of rutile TiO2 photocatalysts via highly n-type F-doping. Journal of Materials Chemistry A, 2014, 2, 3513.	5.2	52
54	Cu–Fe–Se Ternary Nanosheet-Based Drug Delivery Carrier for Multimodal Imaging and Combined Chemo/Photothermal Therapy of Cancer. ACS Applied Materials & Interfaces, 2018, 10, 43396-43404.	4.0	52

#	Article	IF	CITATIONS
55	Cholesterol-Modified Black Phosphorus Nanospheres for the First NIR-II Fluorescence Bioimaging. ACS Applied Materials & Interfaces, 2019, 11, 21399-21407.	4.0	52
56	Controlled Activation of TRPV1 Channels on Microglia to Boost Their Autophagy for Clearance of Alpha‣ynuclein and Enhance Therapy of Parkinson's Disease. Advanced Materials, 2022, 34, e2108435.	11.1	52
57	Semiconductor nanowires for thermoelectrics. Journal of Materials Chemistry, 2012, 22, 22821.	6.7	51
58	In-plane graphene/boron-nitride heterostructures as an efficient metal-free electrocatalyst for the oxygen reduction reaction. Nanoscale, 2016, 8, 14084-14091.	2.8	51
59	Biodegradable Nanoagents with Short Biological Half‣ife for SPECT/PAI/MRI Multimodality Imaging and PTT Therapy of Tumors. Small, 2018, 14, 1702700.	5.2	51
60	Porous Titania Nanosheet/Nanoparticle Hybrids as Photoanodes for Dye-Sensitized Solar Cells. ACS Applied Materials & Interfaces, 2013, 5, 12058-12065.	4.0	50
61	Oral administration of highly bright Cr ³⁺ doped ZnGa ₂ O ₄ nanocrystals for <i>in vivo</i> targeted imaging of orthotopic breast cancer. Journal of Materials Chemistry B, 2018, 6, 1508-1518.	2.9	49
62	Graphiteâ€Nanoplateâ€Coated Bi ₂ S ₃ Composite with Highâ€Volume Energy Density and Excellent Cycle Life for Roomâ€Temperature Sodium–Sulfide Batteries. Chemistry - A European Journal, 2016, 22, 590-597.	1.7	48
63	Threeâ€Stage Interâ€Orthorhombic Evolution and High Thermoelectric Performance in Agâ€Doped Nanolaminar SnSe Polycrystals. Advanced Energy Materials, 2017, 7, 1700573.	10.2	48
64	Overcoming Radioresistance in Tumor Therapy by Alleviating Hypoxia and Using the HIF-1 Inhibitor. ACS Applied Materials & Interfaces, 2020, 12, 4231-4240.	4.0	48
65	The Second Near-Infrared Window Persistent Luminescence for Anti-Counterfeiting Application. Crystal Growth and Design, 2020, 20, 1859-1867.	1.4	46
66	Diluted Magnetic Semiconductor Nanowires Prepared by the Solution–Liquid–Solid Method. Angewandte Chemie - International Edition, 2010, 49, 2777-2781.	7.2	45
67	Effect of polymer ligand structures on fluorescence of gold clusters prepared by photoreduction. Nanoscale, 2013, 5, 1986.	2.8	45
68	On the synergistic effect of hydrohalic acids in the shape-controlled synthesis of anatase TiO ₂ single crystals. CrystEngComm, 2013, 15, 3252-3255.	1.3	45
69	Ambient controlled synthesis of advanced core–shell plasmonic Ag@ZnO photocatalysts. CrystEngComm, 2016, 18, 1713-1722.	1.3	45
70	Synthesis, modification and bioapplications of nanoscale copper chalcogenides. Journal of Materials Chemistry B, 2020, 8, 4778-4812.	2.9	45
71	Biomimetic nanoparticles directly remodel immunosuppressive microenvironment for boosting glioblastoma immunotherapy. Bioactive Materials, 2022, 16, 418-432.	8.6	45
72	CO2 capture and gas separation on boron carbon nanotubes. Chemical Physics Letters, 2013, 575, 59-66.	1.2	40

#	Article	IF	CITATIONS
73	Ambient synthesis of a multifunctional 1D/2D hierarchical Ag–Ag ₂ S nanowire/nanosheet heterostructure with diverse applications. CrystEngComm, 2016, 18, 930-937.	1.3	38
74	Effects of magnetic field strength and particle aggregation on relaxivity of ultra-small dual contrast iron oxide nanoparticles. Materials Research Express, 2017, 4, 116105.	0.8	38
75	Inhibiting autophagy flux and DNA repair of tumor cells to boost radiotherapy of orthotopic glioblastoma. Biomaterials, 2022, 280, 121287.	5.7	38
76	Intravital Multiphoton Imaging of the Selective Uptake of Waterâ€Đispersible Quantum Dots into Sinusoidal Liver Cells. Small, 2015, 11, 1711-1720.	5.2	37
77	The release and detection of copper ions from ultrasmall theranostic Cu _{2â^x} Se nanoparticles. Nanoscale, 2019, 11, 11819-11829.	2.8	37
78	Synthesis and Characterization of Colloidal Core–Shell Semiconductor Nanowires. European Journal of Inorganic Chemistry, 2010, 2010, 4325-4331.	1.0	35
79	Fabrication of Regular ZnO/TiO ₂ Heterojunctions with Enhanced Photocatalytic Properties. Chemistry - A European Journal, 2013, 19, 8393-8396.	1.7	35
80	Effects of nanostructure on clean energy: big solutions gained from small features. Science Bulletin, 2015, 60, 2083-2090.	4.3	35
81	Visualizing Oxidative Stress Level for Timely Assessment of Ischemic Stroke <i>via</i> a Ratiometric Near-Infrared-II Luminescent Nanoprobe. ACS Nano, 2021, 15, 11940-11952.	7.3	35
82	Nanoparticles weaponized with builtâ€in functions for imagingâ€guided cancer therapy. View, 2020, 1, e19.	2.7	35
83	Enhanced thermoelectric performance through synergy of resonance levels and valence band convergence <i>via</i> Q/In (Q = Mg, Ag, Bi) co-doping. Journal of Materials Chemistry A, 2018, 6, 2507-2516.	5.2	34
84	Ultra-Sensitive Detection and Inhibition of the Metastasis of Breast Cancer Cells to Adjacent Lymph Nodes and Distant Organs by Using Long-Persistent Luminescence Nanoparticles. Analytical Chemistry, 2019, 91, 15064-15072.	3.2	32
85	A computational study of carbon dioxide adsorption on solid boron. Physical Chemistry Chemical Physics, 2014, 16, 12695-12702.	1.3	31
86	CO ₂ Capture and Separation from N ₂ /CH ₄ Mixtures by Co@B ₈ /Co@B ₈ [–] and M@B ₉ /M@B ₉ [–] (M = Ir, Rh, Ru) Clusters: A Theoretical Study. Journal of Physical Chemistry A, 2015, 119, 796-805.	1.1	31
87	Reprogramming Tumorâ€Associated Macrophages via ROSâ€Mediated Novel Mechanism of Ultraâ€Small Cu _{2â^'} <i>_x</i> Se Nanoparticles to Enhance Antiâ€Tumor Immunity. Advanced Functional Materials, 2022, 32, 2108971.	7.8	31
88	Ambient Aqueous Growth of Cu ₂ Te Nanostructures with Excellent Electrocatalytic Activity toward Sulfide Redox Shuttles. Advanced Science, 2016, 3, 1500350.	5.6	30
89	Tuning core–shell SiO2@CdTe@SiO2 fluorescent nanoparticles for cell labeling. Journal of Materials Chemistry B, 2013, 1, 2315.	2.9	29
90	Blood Circulation, Biodistribution, and Pharmacokinetics of Dextran-Modified Black Phosphorus Nanoparticles. ACS Applied Bio Materials, 2018, 1, 673-682.	2.3	29

#	Article	IF	CITATIONS
91	Dye-Sensitized Rare Earth-Doped Nanoparticles with Boosted NIR-IIb Emission for Dynamic Imaging of Vascular Network-Related Disorders. ACS Applied Materials & Interfaces, 2021, 13, 29303-29312.	4.0	27
92	Facile Fabrication of Dendritic Mesoporous SiO ₂ @CdTe@SiO ₂ Fluorescent Nanoparticles for Bioimaging. Particle and Particle Systems Characterization, 2016, 33, 261-270.	1.2	26
93	Dyeâ€Sensitized Rare Earth Nanoparticles with Up/Down Conversion Luminescence for Onâ€Demand Gas Therapy of Glioblastoma Guided by NIRâ€II Fluorescence Imaging. Advanced Healthcare Materials, 2022, 11, e2102042.	3.9	26
94	Nitrogen removal from natural gas using solid boron: A first-principles computational study. Fuel, 2013, 109, 575-581.	3.4	23
95	Ambient Synthesis of Oneâ€∕Twoâ€Ðimensional CuAgSe Ternary Nanotubes as Counter Electrodes of Quantumâ€Ðotâ€Sensitized Solar Cells. ChemPlusChem, 2016, 81, 414-420.	1.3	23
96	Size-Dependent Photothermal Conversion and Photoluminescence of Theranostic NaNdF ₄ Nanoparticles under Excitation of Different-Wavelength Lasers. Bioconjugate Chemistry, 2020, 31, 340-351.	1.8	23
97	Solvothermal synthesis and electrochemical properties of S-doped Bi ₂ Se ₃ hierarchical microstructure assembled by stacked nanosheets. RSC Advances, 2016, 6, 38228-38232.	1.7	22
98	Sensitizing the Luminescence of Lanthanide-Doped Nanoparticles over 1500 nm for High-Contrast and Deep Imaging of Brain Injury. Analytical Chemistry, 2021, 93, 7949-7957.	3.2	22
99	Charged-Controlled Separation of Nitrogen from Natural Gas Using Boron Nitride Fullerene. Journal of Physical Chemistry C, 2014, 118, 30006-30012.	1.5	21
100	NIRâ€II Fluorescence imaging for cerebrovascular diseases. View, 2021, 2, 20200128.	2.7	21
101	Controllable synthesis of concave cubic gold core–shell nanoparticles for plasmon-enhanced photon harvesting. Journal of Colloid and Interface Science, 2015, 449, 246-251.	5.0	19
102	Radiolabeled ultra-small Fe ₃ O ₄ nanoprobes for tumor-targeted multimodal imaging. Nanomedicine, 2019, 14, 5-17.	1.7	19
103	Synthesis of magnetic hollow periodic mesoporous organosilica with enhanced cellulose tissue penetration behaviour. Journal of Materials Chemistry, 2011, 21, 7565.	6.7	18
104	An atherosclerotic plaque-targeted single-chain antibody for MR/NIR-II imaging of atherosclerosis and anti-atherosclerosis therapy. Journal of Nanobiotechnology, 2021, 19, 296.	4.2	18
105	Targeted Immunoimaging of Tumorâ€Associated Macrophages in Orthotopic Glioblastoma by the NIRâ€Ib Nanoprobes. Small, 2022, 18, .	5.2	18
106	Xâ€ray investigation of CdSe nanowires. Physica Status Solidi (A) Applications and Materials Science, 2009, 206, 1752-1756.	0.8	17
107	Solution–Liquid–Solid Synthesis of Semiconductor Nanowires Using Clusters as Single ource Precursors. Small, 2011, 7, 2464-2468.	5.2	17
108	Extremely rapid engineering of zinc oxide nanoaggregates with structure-dependent catalytic capability towards removal of ciprofloxacin antibiotic. Inorganic Chemistry Frontiers, 2018, 5, 2432-2444.	3.0	16

#	Article	IF	CITATIONS
109	Cobalt-doped cadmium selenide colloidal nanowires. Chemical Communications, 2011, 47, 11894.	2.2	15
110	Field-effect transistors fabricated from diluted magnetic semiconductor colloidal nanowires. Nanoscale, 2012, 4, 1263.	2.8	15
111	Toward the highly sensitive SERS detection of bio-molecules: the formation of a 3D self-assembled structure with a uniform GO mesh between Ag nanoparticles and Au nanoparticles. Optics Express, 2019, 27, 25091.	1.7	15
112	Insights into the structure-induced catalysis dependence of simply engineered one-dimensional zinc oxide nanocrystals towards photocatalytic water purification. Inorganic Chemistry Frontiers, 2017, 4, 2075-2087.	3.0	14
113	One dimensional hierarchical nanostructures composed of CdS nanosheets/nanoparticles and Ag nanowires with promoted photocatalytic performance. Inorganic Chemistry Frontiers, 2018, 5, 903-915.	3.0	13
114	Activatable Cell-Penetrating Peptide Conjugated Polymeric Nanoparticles with Gd-Chelation and Aggregation-Induced Emission for Bimodal MR and Fluorescence Imaging of Tumors. ACS Applied Bio Materials, 2020, 3, 1394-1405.	2.3	12
115	Copper-Chalcogenide-Based Multimodal Nanotheranostics. ACS Applied Bio Materials, 2020, 3, 6529-6537.	2.3	11
116	Super-Paramagnetic Particles Chemically Bound to Luminescent Diamond: Single Nanocrystals Probed with Optically Detected Magnetic Resonance. Journal of Physical Chemistry C, 2015, 119, 20119-20124.	1.5	9
117	Activatable luminescent probes for imaging brain diseases. Nano Today, 2021, 39, 101239.	6.2	9
118	One-pot aqueous synthesis of cysteine-capped CdTe/CdS core–shell nanowires. Journal of Nanoparticle Research, 2014, 16, 1.	0.8	8
119	Recent Advances in Renal Clearable Inorganic Nanoparticles for Cancer Diagnosis. Particle and Particle Systems Characterization, 2021, 38, 2000270.	1.2	8
120	Photothermal Therapy: Ambient Aqueous Synthesis of Ultrasmall PEGylated Cu _{2â^'} <i>_x</i> Se Nanoparticles as a Multifunctional Theranostic Agent for Multimodal Imaging Guided Photothermal Therapy of Cancer (Adv. Mater. 40/2016). Advanced Materials, 2016, 28, 8788-8788.	11.1	6
121	Boosting the anti-tumor performance of disulfiram against glioblastoma by using ultrasmall nanoparticles and HIF-11 \pm inhibitor. Composites Part B: Engineering, 2022, 243, 110117.	5.9	6
122	Solar Cells: In Situ Growth of a ZnO Nanowire Network within a TiO2Nanoparticle Film for Enhanced Dye-Sensitized Solar Cell Performance (Adv. Mater. 43/2012). Advanced Materials, 2012, 24, 5849-5849.	11.1	5
123	Reprogramming Tumorâ€Associated Macrophages via ROSâ€Mediated Novel Mechanism of Ultraâ€Small Cu _{2â^'} <i>_x</i> Se Nanoparticles to Enhance Antiâ€Tumor Immunity (Adv. Funct.) Tj ET	Qq7181 0.7	′84 3 14 rgB⊺
124	First Observation of Low-Temperature Magnetic Transition in CuAgSe. Journal of Physical Chemistry C, 2018, 122, 19139-19145.	1.5	4
125	Intermittent Starvation Promotes Maturation of Human Embryonic Stem Cell-Derived Cardiomyocytes. Frontiers in Cell and Developmental Biology, 2021, 9, 687769.	1.8	4
126	Boosting Vascular Imagingâ€Performance and Systemic Biosafety of Ultraâ€ s mall NaGdF ₄ Nanoparticles via Surface Engineering with Rationally Designed Novel Hydrophilic Block Coâ€Polymer. Small Methods, 2022, 6, e2101145.	4.6	4

#	Article	IF	CITATIONS
127	Half-sandwich scorpionate nickel complexes with aliphatic dicarboxylic acid co-ligands. Transition Metal Chemistry, 2011, 36, 621-629.	0.7	3
128	Implantable coaxial nanocomposite biofibers for local chemoâ€photothermal combinational cancer therapy. Nano Select, 0, , .	1.9	3
129	Metal Chalcogenides: Thermoelectric Enhancement of Different Kinds of Metal Chalcogenides (Adv.) Tj ETQq1 1 C).784314 i 10 . 2	rgBT /Overlo
130	Ambient Synthesis of Oneâ€∕Twoâ€Dimensional CuAgSe Ternary Nanotubes as Counter Electrodes of Quantumâ€Dotâ€Sensitized Solar Cells. ChemPlusChem, 2016, 81, 352-352.	1.3	2
131	Chemodynamic Therapy: Boosting H ₂ O ₂ â€Guided Chemodynamic Therapy of Cancer by Enhancing Reaction Kinetics through Versatile Biomimetic Fenton Nanocatalysts and the Second Nearâ€Infrared Light Irradiation (Adv. Funct. Mater. 3/2020). Advanced Functional Materials, 2020. 30. 2070019.	7.8	2
132	In vivo static and dynamic angiography of thrombosis by using multi-functional lanthanide nanoprobes. Science Bulletin, 2022, 67, 461-465.	4.3	2
133	Theoretical study on the reaction mechanisms between propadienylidene and R–H (R=F, OH, NH2, CH3): an alternative approach to the formation of alkyne. Structural Chemistry, 2013, 24, 33-38.	1.0	1
134	Scorpionate nickel complexes with dicarboxylic acid ligands: influence of different spanning dicarboxylato co-ligands on the structures. Transition Metal Chemistry, 2012, 37, 553-561.	0.7	0
135	Controlled Activation of TRPV1 Channels on Microglia to Boost Their Autophagy for Clearance of Alpha‣ynuclein and Enhance Therapy of Parkinson's Disease (Adv. Mater. 11/2022). Advanced Materials, 2022, 34, .	11.1	0